

## $^{27}\text{Al}$ NMR, a Quadrupolar Probe for the Entatic State and Stability of Metallochromophores. A Study of Ferrichrome Peptides at 65.1 MHz

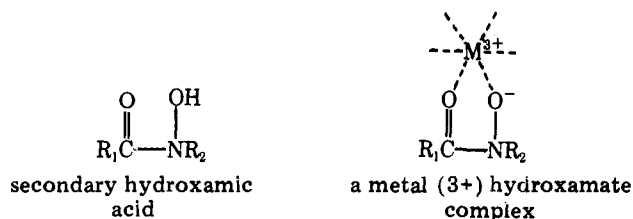
Miguel Llinás\* and Antonio De Marco<sup>1</sup>

Contribution from the Department of Chemistry, Carnegie-Mellon University, Pittsburgh, Pennsylvania 15213. Received July 11, 1979

**Abstract:**  $^{27}\text{Al}$ , a 100% naturally abundant spin  $5/2$  quadrupolar nuclide, exhibits nuclear magnetic resonance (NMR) spectra whose line widths and chemical shifts correlate with the type of coordination and electric field gradients at the metal binding site. Alumichrome, alumichrome C, alumichrome A, and alumichrysin, a set of diamagnetic  $\text{Al}^{3+}$  isomorphous analogues of the naturally occurring ferrichrome siderophores, have been studied by  $^{27}\text{Al}$  NMR at 65.1 MHz. From the rotational correlation time dependence of the line width, as controlled by solvent viscosity changes, we derive values of 33 MHz for the quadrupolar coupling constant and  $1.4 \times 10^{21} \text{ V/m}^2$  for the electrostatic field gradient at the alumichrome C metal binding center. It is shown that a significant contribution to the ligand field asymmetry is intrinsic to the hydroxamate moiety and probably arises from a nonuniform electron charge distribution between the two ligand dentates. The effect is magnified in alumichrome A both by extra charge density and anisotropies on the hydroxamate acyl group, increasing the line width from 1.6 to 6.6 kHz. The  $^{27}\text{Al}$  chemical shift of the trishydroxamate complexes, ca. 41.5 ppm to lower fields from the hexaaquo complex, lies within the characteristic tetrahedral coordination range and removed by about +21 ppm from the known octahedral coordination chemical shift limit. The combined evidence points toward a noncubic ligand field configuration for the ferrichrome peptides.  $^{27}\text{Al}$  NMR enables us to visualize tris-, bis-, and monoacyl hydroxamate coordination derivatives of  $\text{Al}^{3+}$  in equilibrium, at  $\text{pH} < 7$ , with the hexaaquo complex. Resolution enhanced spectra show that similar multiple equilibria are present in alumichrome and alumichrysin and that the extra conformational stability of alumichrysin vis-à-vis alumichrome, as determined by rates of amide  $^1\text{H}$ - $^2\text{H}$  exchange, correlates well with their relative affinities for metal binding.

### Introduction

The ferrichromes integrate a group of biologically active iron transport cyclohexapeptides whose basic structure is shown in Figure 1. Essentially, they consist of a triornithyl sequence followed by a tripeptide of the type  $-\text{NH-Res}^3\text{-Res}^2\text{-Gly}^1\text{-CO-}$ , where  $\text{Res}^{2,3}$  are variable, being glycyl residues in ferrichrome itself and combinations of glycyl, seryl, or alanyl residues in the various homologues.  $\text{Fe}^{3+}$  binding is accomplished through complexation by hydroxamate groups integrated by acylated  $\delta$ -*N*-hydroxyl-L-ornithyl side chains.



X-ray studies have provided the structures of ferrichrome A,<sup>2</sup> ferrichrysin,<sup>3</sup> and ferrichrome<sup>4</sup> to 0.2-Å resolution. The crystallographic models show the metal ion to be octahedrally coordinated by the three hydroxamate bidentate ligands in a  $\Lambda$ -cis configuration. The stereospecificity of the chromophore has been investigated using optical means and cleverly exploited by Raymond and collaborators<sup>5</sup> to derive absolute configurations of other siderochromes of unknown structure. From a biological standpoint, it is still an open question as to the extent to which the topography of the coordination site is recognized by the cell surface receptor involved in the physiological transport process.<sup>5-7</sup>

Solution studies by  $^1\text{H}$ ,  $^{13}\text{C}$ , and  $^{15}\text{N}$  NMR on  $\text{Al}^{3+}$ ,  $\text{Ga}^{3+}$ , and  $\text{Co}^{3+}$  diamagnetic analogues of ferrichrome have demonstrated that the solid-state conformation is maintained in various solvents.<sup>8-11</sup> A variety of spectroscopic studies on the ferric compounds coincide in ascribing a ligand field distorted from perfect cubic symmetry. Thus, ESR,<sup>12</sup> Mössbauer,<sup>13</sup> and far IR<sup>14</sup> characterize the ferric ion as being high spin  $d^5$ , in a "rhombic" ligand field ( $g = 4.3$ ). Since these features have a

posteriori been found in other non-heme iron-containing proteins such as transferrin<sup>15,16</sup> and tetrahedrally coordinated rubredoxin,<sup>17,18</sup> and also in enterobactin,<sup>19</sup> a nonhydroxamate siderophore, it is clear that the origin of the ligand field asymmetry in the ferrichromes deserves further study given the key role played by these compounds as structural models for the interpretation of spectroscopic data on biological iron chromophores.<sup>20</sup>

$^{27}\text{Al}$  is a spin  $5/2$  nucleus of 100% natural isotopic abundance and an intrinsic sensitivity of 0.206 relative to  $^1\text{H}$ . It has a quadrupole moment  $Q = 0.149 \times 10^{-24} \text{ cm}^2$  which interacts with local electric field gradients that couple the nucleus to molecular motions, thus affording an efficient magnetic relaxation mechanism. In the limit of fast motion, the nuclear spin quadrupolar relaxation follows the equation<sup>21</sup>

$$\frac{1}{T_Q} = \frac{1}{T_1} = \frac{1}{T_2} = \frac{3}{40} \left[ \frac{2I + 3}{I^2(2I - 1)} \right] \left( 1 + \frac{\chi^2}{3} \right) \left( \frac{e^2 q Q}{\hbar} \right)^2 \tau \quad (1)$$

where  $T_Q$ ,  $T_1$ , and  $T_2$  are the quadrupolar, spin-lattice, and spin-spin relaxation times, respectively,  $I$  is the nuclear spin,  $eQ$  is the electric quadrupole moment,  $eq$  is the electric field gradient,  $\chi$  gives the deviation of the electric field gradient from axial symmetry,  $\hbar$  is Planck's constant divided by  $2\pi$ , and  $\tau$  is the rotational correlation time. Hence, at constant  $\tau$ , the electric field gradient configuration  $(1 + (\chi^2/3))eq$  determines the quadrupolar relaxation, and thus the line width, of the  $^{27}\text{Al}$  resonance. Indeed, when the symmetry is perfectly cubic, as in the hexaaquo ion  $[\text{Al}^{3+}(\text{H}_2\text{O})_6]^{3+}$ , the  $^{27}\text{Al}$  resonance is a sharp peak of line width  $\sim 3 \text{ Hz}$ .<sup>22</sup> In comparison, under similar, room temperature conditions  $\text{Al}(\text{acac})_3$  and  $[\text{Al}(\text{C}_2\text{O}_4)_3]^{3-}$  exhibit line widths of ca. 100 and 125 Hz, respectively, reflecting a less than perfect cubic field and suggesting that the six-membered ring of the acac complex better accommodates octahedral coordination than does the more constrained five-membered ring oxalate complex.<sup>23</sup> In general, depending on viscosity, it has been observed that high-symmetry octahedral complexes never exceed 100 Hz.<sup>23,24</sup> Hence,  $^{27}\text{Al}$  NMR affords an excellent probe to directly investigate the metal binding site of  $\text{Al}^{3+}$  siderophore

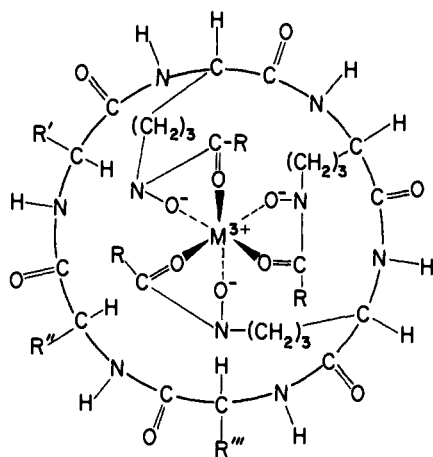


**Figure 1.** Schematic representation of the ferrichrome cyclohexapeptides. M denotes the metal ion,  $\text{Fe}^{3+}$  in the natural products,  $\text{Al}^{3+}$  in the present study. The ferrichrome homologues here discussed differ as indicated in Table I.

derivatives and of other biomolecules where diamagnetic aluminum can substitute for the bioactive metal in an isomorphous fashion.

In this paper we report a  $^{27}\text{Al}$  NMR study of various alumichromes,  $\text{Al}^{3+}$  isomorphous analogues of the ferrichrome peptides (Figure 1), and compare the spectral data with those obtained for tris- $\text{Al}^{3+}$  acetyl hydroxamate. This work represents an attempt to use a quadrupolar NMR nucleus as a probe for active site symmetry in biological compounds and should be of interest for determining the extent of "entasis",<sup>25,26</sup> or distortions at the coordination center due to structural strain imposed by the polypeptide conformation, in metalloproteins.

### Experimental Section

Alumichrome, alumichrome A, alumichrome C, and alumichrysin are from batches already described.<sup>8,9</sup> The tris- $\text{Al}^{3+}$  acetyl hydroxamate complex was formed by dissolving  $\text{AlCl}_3$  in water and adding a slight excess of acetylhydroxamic acid (A grade, Calbiochem). After adjusting to pH 7 with NaOH, the mixture was evaporated and the white solid residue kept under reduced pressure in the presence of  $\text{P}_2\text{O}_5$  until ready for NMR use. The  $[\text{Al}(\text{H}_2\text{O})_6]^{3+}$  standard was generated by dissolving  $\text{Al}_2(\text{SO}_4)_3$  in concentrated  $\text{H}_2\text{SO}_4$ .

The solutions for the NMR studies were prepared with glass doubly distilled water,  $\text{Me}_2\text{SO}-d_6$  (Merck Sharp and Dohme, Canada), or spectroquality 2,2,2-trifluoroethanol (Matheson Coleman and Bell). Sample concentrations were in the range 50–150 mM. All experiments were performed at about 30 °C using 5-mm sample tubes. The spectra were recorded at 65.1 MHz in the correlation mode,<sup>27,28</sup> using the 5.872 T NMR spectrometer of the NIH NMR Facility for Biomedical Research at Carnegie-Mellon University. In dealing with wide-line spectra, fast-scan spectroscopy affords the advantage of efficiently recording the spectrum while the excitation is on, obviating a serious problem of the conventional Fourier approach based on pulsing and then sampling a fast-decaying signal which can result in poor sensitivity. Typically, 200 scans were accumulated per spectrum and, depending on line width, 30–70 kHz were swept in 0.5 s while digitally sampling at a rate of 8190 Hz. Resolution enhancement was based on the optimal filtering window of Ernst.<sup>29</sup>

**Table I.** Alumichrome Homologues<sup>a</sup>

	R'	(site 1)	R''	(site 2)	R'''	(site 3)	ornithyl hydroxamate acyl group: R
alumichrome	-H	(Gly)	-H	(Gly)	-H	(Gly)	-CH <sub>3</sub>
alumichrome C	-H	(Gly)	-CH <sub>3</sub>	(Ala)	-H	(Gly)	-CH <sub>3</sub>
alumichrysin	-H	(Gly)	-CH <sub>2</sub> OH	(Ser)	-CH <sub>2</sub> OH	(Ser)	-CH <sub>3</sub>
alumichrome A	-H	(Gly)	-CH <sub>2</sub> OH	(Ser)	-CH <sub>2</sub> OH	(Ser)	-CH=C(CH <sub>3</sub> )CH <sub>2</sub> COOH

<sup>a</sup> References 5, 8, and 20. R, R', R'', and R''' refer to Figure 1.

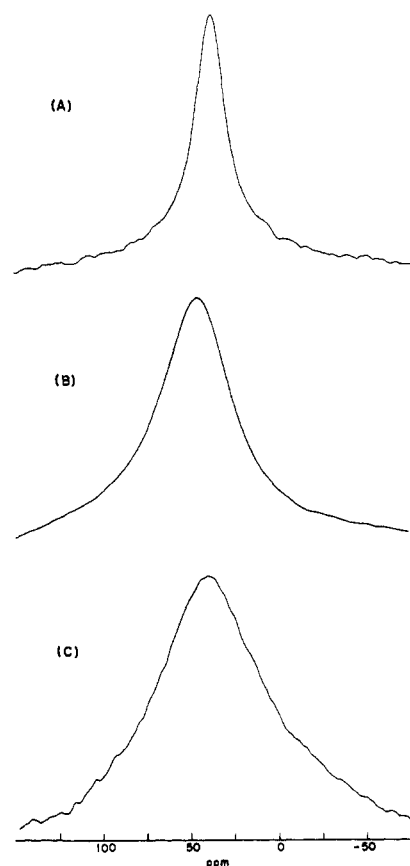


**Figure 2.** 65.14-MHz  $^{27}\text{Al}$  NMR spectra of alumichrome C in various solvents: (A)  $\text{H}_2\text{O}$ , (B) trifluoroethanol, (C)  $\text{Me}_2\text{SO}-d_6$ ,  $t \approx 30$  °C.

### Results and Discussion

Figure 2 shows the  $^{27}\text{Al}$  resonance of alumichrome C, a ferrichrome homologue where an L-alanyl residue substitutes for Gly<sup>2</sup> in alumichrome (Figure 1), in various solvents. The resonance appears at  $\sim 41.5$  ppm downfield from the hexaquo  $^{27}\text{Al}$  resonance, here taken as 0 ppm reference line. As noticed, the chemical shift is little affected by the solvent changes. In contrast, the resonance line width, 1.4 kHz in  $\text{H}_2\text{O}$  solution, increases to 3.2 kHz in trifluoroethanol and even further to 4.7 kHz in  $\text{Me}_2\text{SO}$ . We interpret this effect as being caused by solvent viscosity effects only, as the quadrupolar line width  $1/T_Q \propto \tau$ , the rotational correlation time, and, according to the Stokes-Einstein relation,  $\tau = V\eta/KT$ , where  $V$  is the molecular volume and  $\eta$  is the viscosity of the medium.

At 45 °C, the rotational correlation time of alumichrome in  $\text{Me}_2\text{SO}-d_6$  has been determined to be  $\approx 4 \times 10^{-10}$  s.<sup>30</sup> Accounting for the viscosity changes<sup>31</sup> on lowering the temperature from 45 ( $\eta = 1.51$  cP) to 30 °C ( $\eta = 2.00$  cP) and, at this temperature, on varying the solvent from  $\text{Me}_2\text{SO}$  to  $\text{H}_2\text{O}$  ( $\eta = 0.80$  cP)<sup>32</sup> or to trifluoroethanol ( $\eta \approx 1.57$  cP),<sup>33</sup> we can estimate  $\tau$  for the peptide dissolved in the three solvents at 30 °C. Thus, we obtain  $\tau = 2.2 \times 10^{-10}$  ( $\text{H}_2\text{O}$ ),  $4.4 \times 10^{-10}$

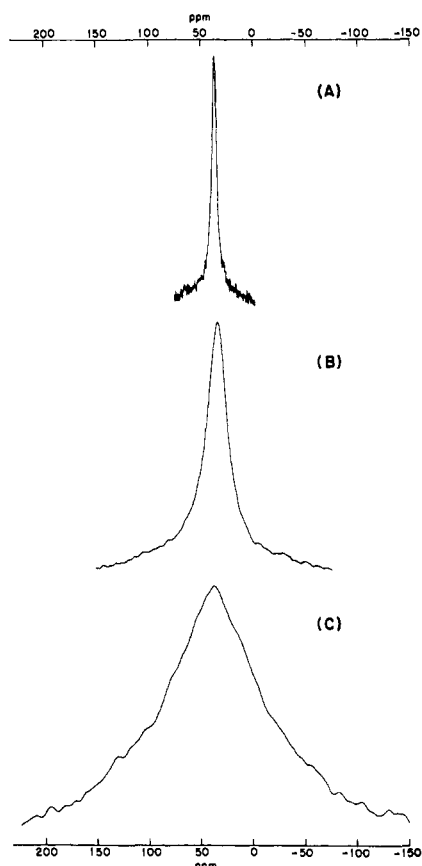


**Figure 3.** (A) 65.14-MHz  $^{27}\text{Al}$  NMR spectra of aluminum tris(acetylhydroxamate) (mol wt 249), (B) alumichrysin (mol wt 771), and (C) alumichrome A (mol wt 1020) in aqueous solution, pH 7. At this pH, alumichrome A is a trianion while alumichrysin is electrically neutral.

(TFE), and  $5.6 \times 10^{-10}$  s ( $\text{Me}_2\text{SO}-d_6$ ), which shows that even in the most viscous of the three solvents  $\omega^2\tau^2 \ll 1$ , so that the extreme narrowing approximation (eq 1) is satisfied for  $^{27}\text{Al}$  at 65.1 MHz. Since  $T_2 = (\pi\delta\nu)^{-1}$ , where  $\delta\nu$  is the line width at half height, we can derive  $T_2$  values in each solvent and linearly fit  $(T_2)^{-1}$  vs.  $\tau$ , as indicated by eq 1. By linear regression we obtain a slope of  $2.604 \times 10^{13} \text{ s}^{-2}$  (correlation coefficient  $r = 0.99$ ) and, substituting  $l = 5/2$  into eq 1, we derive 32.9 MHz for the quadrupolar coupling constant  $(1 + \chi^2/3)^{1/2}e^2qQ/\hbar$ . Considering that the line width is proportional to the square of this magnitude, this value appears quite reasonable; e.g., for  $^{27}\text{Al}(\text{H}_2\text{O})_6$  the quadrupolar coupling constant has been estimated<sup>23</sup> to be 1 MHz. Remembering that for  $^{27}\text{Al}$   $Q = 0.149 \times 10^{-24} \text{ cm}^2$ , we can herefrom derive a value for the field gradient of  $1.45 \times 10^{21} \text{ V/m}^2$  that provides a quantitative estimate of the extent of ligand field asymmetry at the metal ion center.

Figure 3A shows the resonance of aluminum tris(acetylhydroxamate), a low molecular weight derivative that serves as a valuable model compound. In  $\text{H}_2\text{O}$ , pH 7, the trihydroxamate  $^{27}\text{Al}$  resonance appears at 36.55 ppm, i.e., not too shifted from the alumichrome peptides' signals. Its line,  $\sim 370$  Hz wide, is considerably sharper than that of the Ser<sup>2</sup>, Ser<sup>3</sup> alumichrome homologue alumichrysin ( $\delta\nu = 1.6$  kHz, Figure 3B). Alumichrysin has 771 molecular weight, i.e., it is 3.1 times heavier than aluminum tris(acetylhydroxamate). Assuming isotropic tumbling, the molecular size effect on  $\tau$  predicts about 1.1 kHz for the line width of the alumichrysin  $^{27}\text{Al}$  resonance. The 0.5-kHz discrepancy with the measured value suggests an extra contribution to the ligand field anisotropy stemming from structural constraints imposed by the peptide conformation, i.e., due to *entasis*. However, the fact that a simple, unconstrained hydroxamate shows a considerable line breadth in-

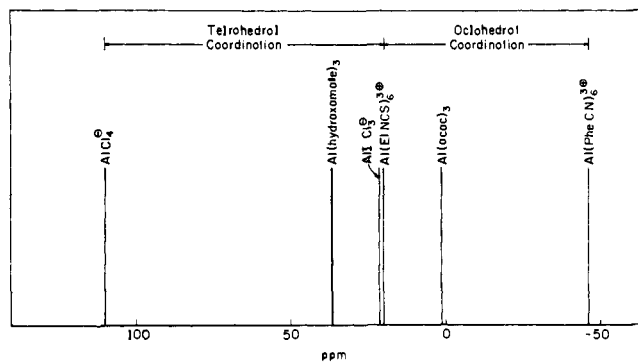


**Figure 4.** Effect of coordination on the  $^{27}\text{Al}$  resonance chemical shift. The hydroxamate chemical shift was determined in this study. Other resonance positions have been extracted from Akitt.<sup>24</sup> Notice the unusual position of the octahedral trihydroxamate complex, *within* the tetrahedral chemical shift range. Chemical shifts are given in parts per million, to lower fields from the  $[\text{Al}(\text{H}_2\text{O})_6]^{3+}$  peak.

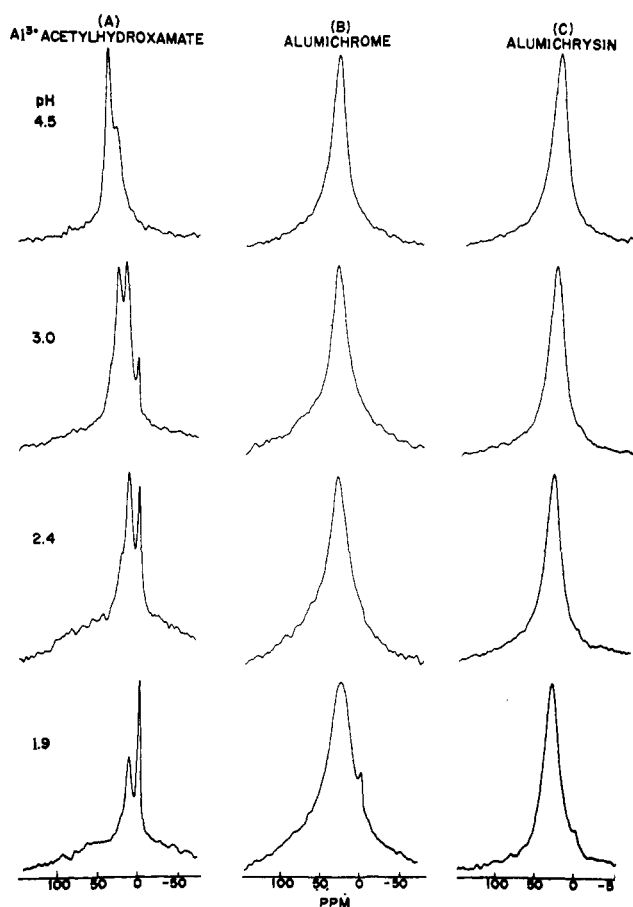
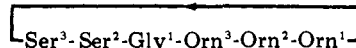


**Figure 5.** Acidity effects on the  $^{27}\text{Al}$  resonance positions: aluminum tris(acetylhydroxamate) (A), alumichrome (B), and alumichrysin (C).

icates that electric field gradients present in the alumichromes already exist in the hydroxamate ligand and that, by this criterion, the peptide moiety is not the most significant factor distorting the octahedral coordination.

The subtle control of the  $^{27}\text{Al}$  line width by local electric fields is dramatized by comparing the spectrum of alumichrysin ( $\delta\nu = 1.6$  kHz, Figure 3B) and alumichrome A ( $\delta\nu = 6.6$  kHz, Figure 3C). Both peptides possess the same amino acid sequence, namely,



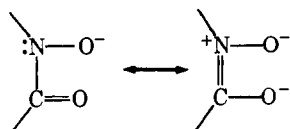
but differ in the nature of the side-chain hydroxamate acyl moiety, which is an acetyl group in case of alumichrysin (and

**Table II.** Crystallographic Metal–Oxygen Bond Distances for Various Hydroxamates<sup>a</sup>

	M–ON	M–OC
Cr(benz) <sub>3</sub> <sup>b,c</sup>	1.960 (4)	1.984 (5)
Fe(benz) <sub>3</sub> <sup>b,d</sup>	1.980 (5)	2.051 (10)
ferrioxamine E <sup>e</sup>	1.953 (9)	2.055 (2)
ferrichrome <sup>f</sup>	1.983 (10)	2.034 (6)
ferrichrysin <sup>g</sup>	1.974 (7)	2.061 (20)
ferrichrome A <sup>f,h</sup>	1.980 (11)	2.033 (11)
alumichrome A <sup>f</sup>	1.883 (8)	1.907 (10)

<sup>a</sup> Mean values, in Å units. Standard deviations for the least significant figure are given in parentheses. <sup>b</sup> Benzhydroxamate. <sup>c</sup> Reference 36. <sup>d</sup> Reference 35. <sup>e</sup> Reference 34. <sup>f</sup> Reference 37. <sup>g</sup> Reference 3. <sup>h</sup> Reference 2.

of all other alumichromes except alumichrome A), and *trans*- $\beta$ -methylglutaconic acid, totally ionized at pH 7, in the case of alumichrome A. We propose that this excess of three electronic charges is affecting the electric field gradient through anisotropy in the extra charge distribution.  $^{27}\text{Al}$  NMR is thus effectively sensing the lack of cubic symmetry of the ligand field and the distortions predicted by other spectroscopies centered on the ferric chromophore.<sup>12–14</sup> Furthermore, this nonuniform charge distribution fundamentally arises from the hydroxamate moiety, which preferentially concentrates electron density on the N–O<sup>–</sup> over the C=O dentate:



Assuming a purely ionic ligand–metal (L–M) interaction, the higher polarizability of the NO<sup>–</sup> group would shorten the NO<sup>–</sup>–M distance relative to the CO–M distance. This would result in trigonal distortion, which has been observed in crystallographic studies of ferrichromes,<sup>2–4</sup> in ferrioxamine E,<sup>34</sup> and in simple hydroxamates<sup>35,36</sup> (Table II). Abu-Dari et al.<sup>36</sup> have discussed these structural data in some detail.

Further support to the above interpretation is provided by the aluminum tris(hydroxamate) chemical shift. As observed by Haraguchi and Fujiwara,<sup>23</sup> the position of the  $^{27}\text{Al}$  resonance correlates well with the type of coordination of the Al<sup>3+</sup> ion. Thus, octahedral complexes extend from about –46 to +20 ppm while tetrahedral derivatives span the region from about +21 to +110 ppm.<sup>24</sup> As indicated in Figure 4, the hydroxamate signals at ca. 37 ppm lie outside the expected octahedral coordination range, which suggests, again, that the metal ion is not sensing a strict octahedral field.

$^{27}\text{Al}$  NMR affords the possibility of studying relative stabilities of the various alumipectides. As illustrated in Figure 5, on going from pH 4.5 to 3.0, the number of acetylhydroxamate  $^{27}\text{Al}$  spectral lines changes from two to four. The multiplicity of peaks in the acidic pH range is due to partial protonation of hydroxamate groups ( $\rightarrow$  hydroxamic acid) with a simultaneous displacement from the coordination sphere and substitution by H<sub>2</sub>O ligands. Thus, on acidifying, the singlet at pH 7 due to the trihydroxamate species (Figure 3A) decreases its intensity at pH 4.5, while a neighbor peak now appears at higher fields, due to generation of the [Al–dihydroxamate–(H<sub>2</sub>O)<sub>2</sub>]<sup>+</sup> complex and eventually it almost disappears at pH 3.0, due to predominance of the bis- and monohydroxamate derivatives, with some formation of the hexaaquo complex. These peaks shift to higher fields as the extent of H<sub>2</sub>O coordination is increased. Further acidification generates more of the monohydroxamate and the hexaaquo species. In contrast, alumichrome (B) and alumichrysin (C) show no pH effect, preserving their pH 7 line widths of ca. 1.6 kHz down to pH 3.0. As the acidity is further increased,

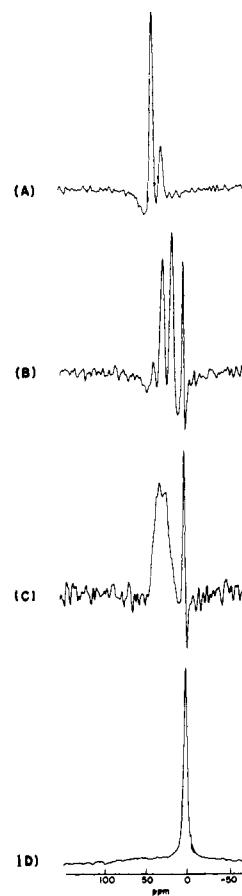


**Figure 6.** Resolution-enhanced spectra from Figure 5: (A) Al<sup>3+</sup> acetylhydroxamate, pH 4.5; (B) Al<sup>3+</sup> acetylhydroxamate, pH 3.0; (C) alumichrome, pH 1.9; (D) Al<sub>2</sub>(SO<sub>4</sub>)<sub>3</sub> dissolved in H<sub>2</sub>SO<sub>4</sub>, pH 2.4. (B) illustrates the coexistence, at pH 3.0, of hexaaquomono-, di-, and trihydroxamate Al<sup>3+</sup> complexes in the acetylhydroxamate derivatives. Notice the mixture of resonances in the alumichrome spectrum at pH 1.9 (C), coexisting with the well-resolved line of the hexaaquo ion at 0 ppm. (D) shows the resonance of Al(H<sub>2</sub>O)<sub>6</sub><sup>3+</sup>, without digital filtering.

however, the alumichrome apparent line width increases to 2.2 kHz at pH 2.4, without significant concomitant effect on the alumichrysin resonance. These alumipectides differ only in the occupancy of sites 2 and 3 (Figure 1, Table I) which are filled in by glycyl residues, in alumichrome and by L-seryl residues in alumichrysin. Thus, although the two isomorphous cyclic peptide–hydroxamates are significantly more stable than the triacetyl hydroxamate complexes (entropic “chelate” effect), the broadening of the alumichrome resonance at pH 2.4 is suggestive of a lesser stability of this peptide relative to alumichrysin, solely due to their *subtly different amino acid compositions*. The broadening would thus be due to coexistence, in alumichrome, of several coordination species that differ in the extent of H<sub>2</sub>O participation, possibly in relatively fast exchange. As the acidity is further increased to pH 1.9, a shoulder peak appears at 0 ppm in alumichrome and, to a lesser extent, in alumichrysin, due to formation of the hexaaquo Al<sup>3+</sup> complex. The different affinities for metal coordination exhibited by the two peptides correlate with their different conformational stabilities as measured by rates of amide NH <sup>1</sup>H–<sup>2</sup>H exchange in <sup>2</sup>H<sub>2</sub>O solutions, where alumichrysin shows rates of isotopic exchange that are significantly smaller than for alumichrome.<sup>20</sup> It would thus appear that metal coordination and conformational fluctuations are intimately related, lower affinities for metal binding corresponding to larger amplitudes of structural breathing.

Total resolution of the various Al<sup>3+</sup> complexes can be achieved by digital filtering matched to the pathological line widths (Figure 6). We notice that, while the tri- and dihyd-

roxamate complexes are present in the acetylhydroxamate complexes at pH 4.5 (A) and 3.0 (B), the monohydroxamate and the hexaquo complexes coexist at the lower pH (B). By comparison, the resolution enhanced spectrum of aluminichrome at pH 1.9 (C) strongly suggests equilibration between these three species plus a significant displacement toward the hexaquo ion, shown as a reference, without digital filtering, in Figure 6D.

This study represents a first instance of the use of  $^{27}\text{Al}$  NMR spectroscopy to derive direct information on (a) electric field gradients at metal coordination centers in biomolecules and (b) metal-binding affinity differences among homologous structures with common metal-binding sites. Since for a given ligand field configuration the line breadth increases with the molecular weight, the use of  $^{27}\text{Al}$  NMR as a quadrupolar probe for metalloproteins should prove to be informative mainly in cases of high symmetry. For small peptides, as studied here, the technique provides a quantitative basis to ascertain the extent of entasis at the active site.

**Acknowledgments.** This research was partially supported by the donors of the Petroleum Research Fund, administered by the American Chemical Society, and by the National Institutes of Health, Grant GM25213. The NMR facility is supported by NIH Grant RR 00292.

## References and Notes

- (1) NATO Senior Fellow. Istituto di Chimica delle Macromolecole, Consiglio Nazionale delle Ricerche, Via A Corti 12, 20133 Milano, Italy.
- (2) A. Zalkin, J. D. Forrester, and D. H. Templeton, *J. Am. Chem. Soc.*, **88**, 1810-1814 (1966).
- (3) R. Norrestam, B. Stensland, and C. I. Brändén, *J. Mol. Biol.*, **99**, 501-506 (1975).
- (4) R. A. Lohry and D. van der Helm, Abstracts, American Crystallographic Association Winter Meeting, March 1978, No. PB2.
- (5) K. N. Raymond and C. Carrano, *Acc. Chem. Res.*, **12**, 183-190 (1979).
- (6) J. Leong and J. B. Neilands, *J. Bacteriol.*, **126**, 823-830 (1976).
- (7) C. J. Carrano and K. N. Raymond, *J. Bacteriol.*, **136**, 69-74 (1978).
- (8) M. Llinás and J. B. Neilands, *Biophys. Struct. Mech.*, **2**, 105-117 (1976).
- (9) M. Llinás, D. M. Wilson, and M. P. Klein, *J. Am. Chem. Soc.*, **99**, 6846-6850, 8374 (1977).
- (10) M. Llinás and K. Wüthrich, *Biochim. Biophys. Acta*, **532**, 29-40 (1978).
- (11) A. De Marco and M. Llinás, *Biochemistry*, **18**, 3846-3854 (1979).
- (12) H. H. Wickman, M. P. Klein, and D. A. Shirley, *J. Chem. Phys.*, **42**, 2113-2117 (1965).
- (13) H. H. Wickman, M. P. Klein, and D. A. Shirley, *Phys. Rev.*, **152**, 345-357 (1966).
- (14) G. C. Brackett, P. L. Richards, and W. S. Gaughey, *J. Chem. Phys.*, **54**, 4383-4401 (1971).
- (15) R. Aasa, *Biochem. Biophys. Res. Commun.*, **49**, 806-812 (1972).
- (16) R. A. Pinkowitz and P. Aisen, *J. Biol. Chem.*, **247**, 7830-7834 (1972).
- (17) W. Lovenberg in "Peptides of the Biological Fluids", Vol. 14, H. Peeters, Ed., Elsevier, Amsterdam, 1966, pp 165-172.
- (18) D. J. Newman and J. R. Postgate, *Eur. J. Biochem.*, **7**, 45-50 (1968).
- (19) I. G. O'Brien, G. B. Cox, and F. Gibson, *Biochim. Biophys. Acta*, **237**, 537-549 (1971).
- (20) M. Llinás, *Struct. Bonding (Berlin)*, **17**, 135-220 (1973).
- (21) A. Abragam, "The Principles of Nuclear Magnetism", Pergamon Press, Oxford, 1961, Chapter VIII.
- (22) F. W. Wehrli in "Nuclear Magnetic Resonance of Less Common Nuclei", 15th Varian NMR Workshop, Zürich, 1975, pp 25-33.
- (23) H. Haraguchi and S. Fujiwara, *J. Phys. Chem.*, **73**, 3467-3473 (1969).
- (24) J. W. Akitt, *Annu. Rep. NMR Spectrosc.*, **5A**, 466-556 (1972).
- (25) B. L. Vallee and R. J. P. Williams, *Proc. Natl. Acad. Sci. U.S.A.*, **59**, 498-505 (1968).
- (26) R. J. P. Williams, *Cold Spring Harbor Symp. Quant. Biol.*, **36**, 53-62 (1971).
- (27) J. Dadok and R. F. Sprecher, *J. Magn. Reson.*, **13**, 243-248 (1974).
- (28) R. K. Gupta, J. A. Ferretti, and E. D. Becker, *J. Magn. Reson.*, **13**, 275-290 (1974).
- (29) R. E. Ernst, *Adv. Magn. Reson.*, **2**, 1-135 (1966).
- (30) M. Llinás, M. P. Klein, and K. Wüthrich, *Biophys. J.*, **24**, 849-862 (1978).
- (31) H. L. Schäfer and W. Schaffernicht, *Angew. Chem.*, **72**, 618-626 (1960).
- (32) R. C. Weast, Ed., "Handbook of Chemistry and Physics", 52nd ed., Chemical Rubber Publishing Co., Cleveland, 1971, p F36.
- (33) "Trifluoroethanol", Halocarbon Products Corp., Hackensack, N.J., 1967.
- (34) D. van der Helm and M. Poling, *J. Am. Chem. Soc.*, **98**, 82-86 (1976).
- (35) V. H. J. Lindner and S. Gottlicher, *Acta Crystallogr., Sect. B*, **25**, 832, 842 (1969).
- (36) K. Abu-Dari, J. D. Ekstrand, D. P. Freyberg, and K. N. Raymond, *Inorg. Chem.*, **18**, 108-112 (1979).
- (37) D. van der Helm, unpublished. See ref 4.

## The Effect of Spin Saturation on Nuclear Overhauser Effects

Joseph H. Noggle

Contribution from the Department of Chemistry, University of Delaware, Newark, Delaware 19711. Received July 30, 1979

**Abstract:** In homonuclear magnetic resonance, measurement of nuclear Overhauser effects (both transient and steady state) is affected by indirect saturation of the observed resonance if the chemical shift between the spin being irradiated and the spin observed is not very large compared to the rf power. This problem is discussed theoretically and practical formulas are derived to correct experimental results for the effect of partial saturation. Transient effects (Torrey oscillations) are also discussed.

## Introduction

The nuclear Overhauser effect (NOE) has become a powerful and commonly used tool for the determination of molecular conformations and configurations and for the assignment of nuclear magnetic resonance (NMR) spectra. Formulas used for the interpretation of such measurements in both steady-state<sup>1</sup> and transient<sup>2</sup> experiments generally ignore the indirect saturation of the observed resonance due to the nearby off-resonance rf field, in effect assuming an infinite chemical shift between the irradiated and the observed spins. This convenient set of circumstances does not always hold true. In this paper, the theory of these indirect saturation effects is discussed for a two-spin system and conclusions are drawn which will be of help in multispin systems.

## Theory

We start with the set of coupled Bloch equations for the spins:

$$dU_i/dt + \sum_j R_{ij}U_j = -\Delta_i V_i \quad (1)$$

$$dV_i/dt + \sum_j R_{ij}V_j = \Delta_i U_i + \omega_1 M_{zi} \quad (2)$$

$$dM_{zi}/dt + \sum_j \Gamma_{ij}(M_{zj} - M_{0j}) = -\omega_1 V_i \quad (3)$$

where  $\omega_1 = \gamma H_1$ , the rf field power, and  $\Delta_i = \omega_i - \omega_0$ , the difference between the resonance frequency of spin  $i$  and the Larmor frequency,  $\omega_0 = \gamma H_0$ . Formulas for the spin-lattice